

CONFINEMENT AND SCALING IN DEEP INELASTIC PROCESSES *

S.A. Gurvitz

Department of Particle Physics, Weizmann Institute of Science, Rehovot 76100, Israel

The existing data for hadron structure functions, $F_2(x, Q^2)$, show considerable Q^2 -dependence, which is mainly attributed to the QCD logarithmic corrections to Bjorken scaling. However, at $x \rightarrow 1$ the scaling violations are dominated by power corrections $\propto 1/Q^2$ (higher twist and target mass effects):

$$F_2(x, Q^2) = F_2^{as}(x, Q^2) + \frac{B(x)}{Q^2} + \dots, \quad (1)$$

where $F_2^{as}(x, Q^2) = F_2(x, Q^2 \gg |B(x)|)$ and the remaining Q^2 -dependence in $F_2^{as}(x, Q^2)$ is to be attributed to QCD logarithmic corrections only.

Power corrections can be incorporated in the first term of Eq. (1) by using a different scaling variable,

$$\hat{x} = \phi(x, Q^2) = x + \frac{b(x)}{Q^2} + \dots, \quad (2)$$

so that

$$F_2(x, Q^2) = F_2(\phi^{-1}(\hat{x}, Q^2), Q^2) \simeq F_2^{as}(\hat{x}, Q^2). \quad (3)$$

The coefficient B , which determines the value of the power correction in Eq. (1), is thus related to the structure function by $B(x) = b(x) \partial F_2^{as}(x, Q^2) / \partial x$. In fact, an analysis of data in terms of an appropriate scaling variable appears to be more convenient, than the direct evaluation of power corrections.

*WIS-97/2/Jan.-PH. Invited paper given at ISHEPP, Dubna, September 1996.

In general, the power corrections are generated by confining interaction of partons in the final state. At first sight, such an interaction should influence the structure function very drastically. Consider for instance the example of two *nonrelativistic* “quarks” of mass m interacting via a harmonic oscillator potential [1]. These quarks are never free and therefore the system in the final state possesses a discrete spectrum. As a result the structure function, $F(q, \nu)$, as a function of the energy transfer ν , is given by a sum of δ - functions. Obviously, it looks very different from the structure function obtained in the impulse approximation, which considers the struck parton as a free particle in the final state. This paradox can be resolved by introducing a (nonrelativistic) scaling variable y

$$y = -\frac{|\mathbf{q}|}{2} + \frac{m\nu}{|\mathbf{q}|}, \quad (4)$$

Then expanding the structure function $\mathcal{F}(q, y) \equiv F(q, \nu)$ in powers of $1/q$, one finds in the limit $q \rightarrow \infty$ and $y = \text{const}$ that the δ -peaks merge to a smooth curve, $\mathcal{F}(q, y) \rightarrow \mathcal{F}_0(y)$, which coincides with a free parton response [2]. Although this result appears to confirm the parton model picture, it does not imply that the interaction in the final state is not important. The latter has been merely incorporated in $\mathcal{F}_0(y)$ by an appropriate choice of the scaling variable y , as shown by Eqs. (1-2). The remaining contribution from higher-order ($\sim 1/q$) terms are thus minimized. However, a non-optimal choice of the scaling variable could result in very large or even singular corrections to the structure function. One can anticipate that an appropriate choice of the scaling variable is especially relevant at large x , where lower-lying excitations should play an important role.

A general analysis performed in the framework of Bethe-Salpeter equation shows that in an analogy with the nonrelativistic case [1,2] the higher twist terms from a local confining final state interaction and target mass effects can be effectively accounted in the modified the struck quark propagator, where the quark mass has the same off-shell value before and after the virtual photon absorption [3],

FIGURES

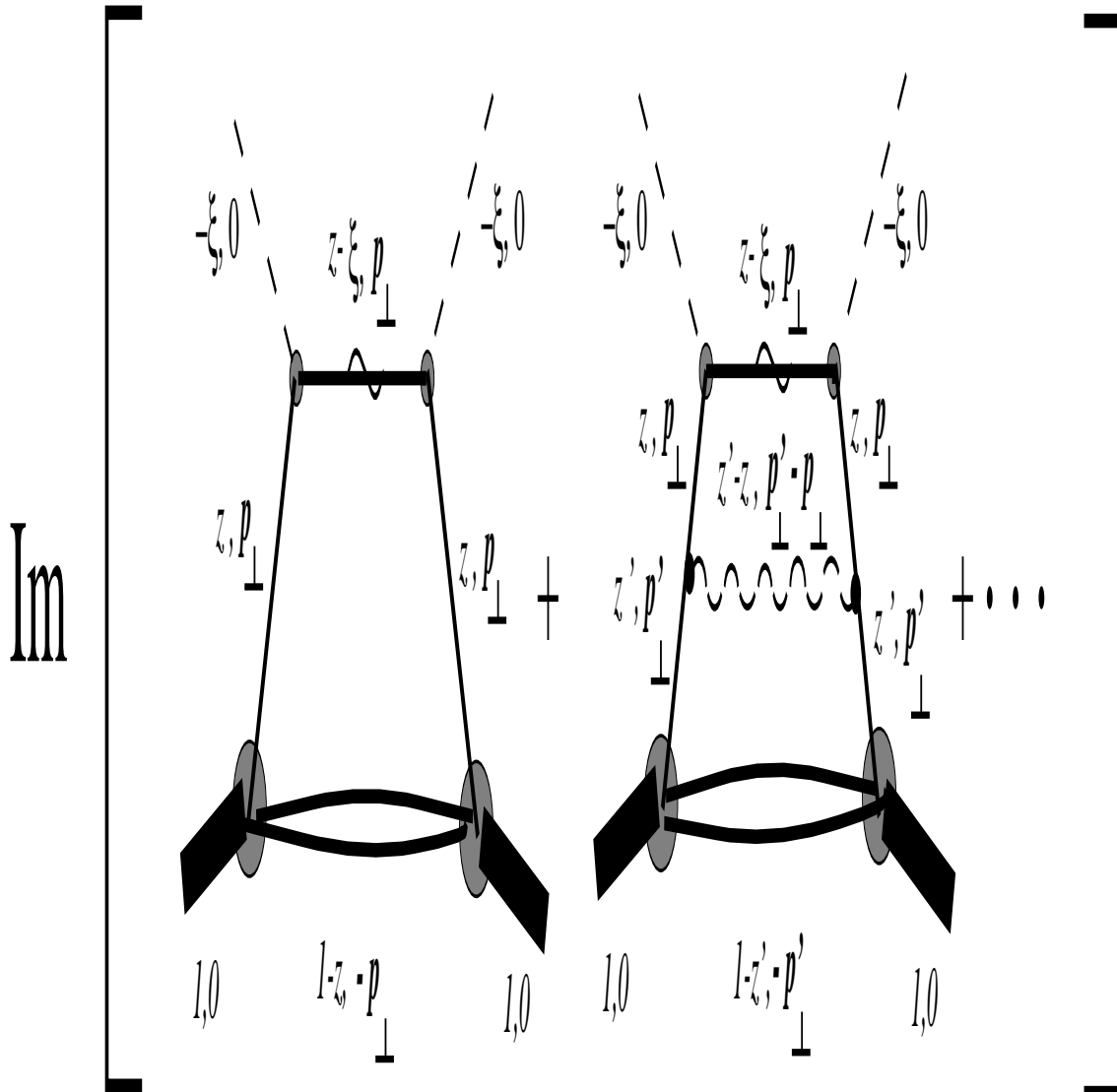


FIG. 1. Diagrammatic representation of the leading contributions to the structure function using light-cone variables. Quarks and gluons are shown by solid and wavy lines respectively. The modified propagators are marked by “ \sim ”.

As a result, the Bjorken scaling variable x is replaced by a new scaling variable $\bar{x} \equiv \bar{x}(x, Q^2)$, which is the light-cone fraction of the *off-shell* struck quark. Explicitly,

$$\bar{x} = \frac{x + \sqrt{1 + 4M^2x^2/Q^2} - \sqrt{(1-x)^2 + 4m_s^2x^2/Q^2}}{1 + \sqrt{1 + 4M^2x^2/Q^2}}, \quad (5)$$

where M is the target mass and m_s is the invariant mass of spectator partons (quarks and

gluons). For $Q^2 \rightarrow \infty$ or for $x \rightarrow 0$ the variable \bar{x} coincides with the Bjorken variable x . However, at finite Q^2 these variables are quite different.

It follows from Eq. (5) that \bar{x} depends on the invariant spectator mass, m_s . In terms of light-cone variables, Fig. 1, it can be written as

$$m_s^2 = m_0^2 + (1 - z) \frac{(\mathbf{p}'_{\perp} - \mathbf{p}_{\perp})^2}{z' - z} + (z' - z) \frac{m_0^2 + \mathbf{p}'^2}{1 - z'} + \mathbf{p}'_{\perp}{}^2 - \mathbf{p}_{\perp}{}^2, \quad (6)$$

where m_0 is the diquark mass, and $1 \geq z' \geq z$. We approximate m_s as an effective spectator mass depends only on external momenta. Since $z \rightarrow \bar{x} \simeq x$ and $z' \sim z$, one gets from Eq. (6)

$$m_s^2 \simeq m_0^2 + C(x, Q^2)(1 - x) \quad (7)$$

Eq. (7) for the invariant spectator mass looks quite appealing apart from its relation to Eq. (6). Indeed, $x = 1$ corresponds to elastic scattering, when no gluons are emitted. Therefore in this case the spectator is represented by a diquark. When x decreases, gluons are emitted and m_s^2 increases $\propto (1 - x)$. The coefficient $C(x, Q^2)$ in Eq. (7) determines the rate of increase of the spectator mass with Q^2 and x . It can be found self-consistently from the evolution equation. However, when $x \sim 1$, one can take $C(x, Q^2) \simeq C(1, Q^2) \simeq \text{const}$, because of Q^2 -dependence of the spectator mass is less important than its x -dependence near the elastic threshold. We roughly estimated the value of C by using the Weizsäcker-Williams or “equivalent photon” approximation, utilized in Ref. [4] for derivation of the evolution equation. One finds from [4] that the light-cone fraction of the “equivalent” gluon, $z - z'$, (Fig. 1) is of order $\alpha_s \ln(Q^2/Q_0^2)$ in the region of large x . However, the probability of the gluon emission is also about the same order of magnitude. Then, as follows from Eq. (6), $C \sim \langle (\mathbf{p}'_{\perp} - \mathbf{p}_{\perp})^2 \rangle$, so that one could expect to find C on the scale of $(\text{GeV})^2$. In the following we regard it as a phenomenological parameter, determined from the data.

Let us consider the nucleon structure functions in the region of large x , where the power corrections to the scaling are dominant. At present, the only available large- x data for proton and deuteron structure functions, $F_2^p(x, Q^2)$, $F_2^d(x, Q^2)$, are the SLAC data [5–8],

taken at moderate values of momentum transfer, $Q^2 < 30 \text{ (GeV/c)}^2$. (The nucleon structure functions for higher values of momentum transfer ($Q^2 \leq 230 \text{ (GeV/c)}^2$) are extracted from BCMDS [9] and NMC [10] data, yet only for $x \leq 0.75$). The SLAC data for the proton and deuteron structure functions for $x \geq 0.7$ and $5 < Q^2 < 30 \text{ (GeV/c)}^2$ are shown in Fig. 2 as a function of x . Also shown is the value of $F_2^p(x, Q^2)$ and $F_2^d(x, Q^2)$ for $Q^2 = 230 \text{ (GeV/c)}^2$ and $x = 0.75$ taken from the BCDMS data [9]. The data points close to the region of resonances were excluded by a requirement that the invariant mass of the final state $(M + \nu)^2 - \mathbf{q}^2$ is greater than $(M + \Delta)^2$, where $\Delta = 300 \text{ MeV}$. In addition, we excluded the data points with $x > 0.9$ from the deuteron structure only (Fig. 2b). The reason is that the deuteron structure function can not be represented as an average of the proton and neutron structure functions for $x > 0.9$. Indeed, the calculations of Melnitchouk *et al.* [11] show that the ratio $2F_2^d/(F_2^p + F_2^n)$ is about 1.13 for $x = 0.9$ and $Q^2 = 5 \text{ (GeV/c)}^2$, and it rapidly increases for $x > 0.9$. However, for $x < 0.85$, this ratio is within 5% of unity [12].

One finds from Fig.2 that the structure functions show no scaling in the Bjorken variable x . Also, very poor scaling is obtained when the data are plotted as a function of the Nachtmann variable ξ [8]. However, the situation is different if we display the same data as a function of the variable \bar{x} , Eq. (5). It appears that the scaling in the \bar{x} -variable is strongly dependent on the value of diquark mass, m_0 , Eq. (7), but is much less sensitive to variation of the coefficient C . For instance, the data as a function of \bar{x} display very poor scaling for $m_0 > 600 \text{ MeV}$, i.e. by considering the spectator as build up from constituent quarks.

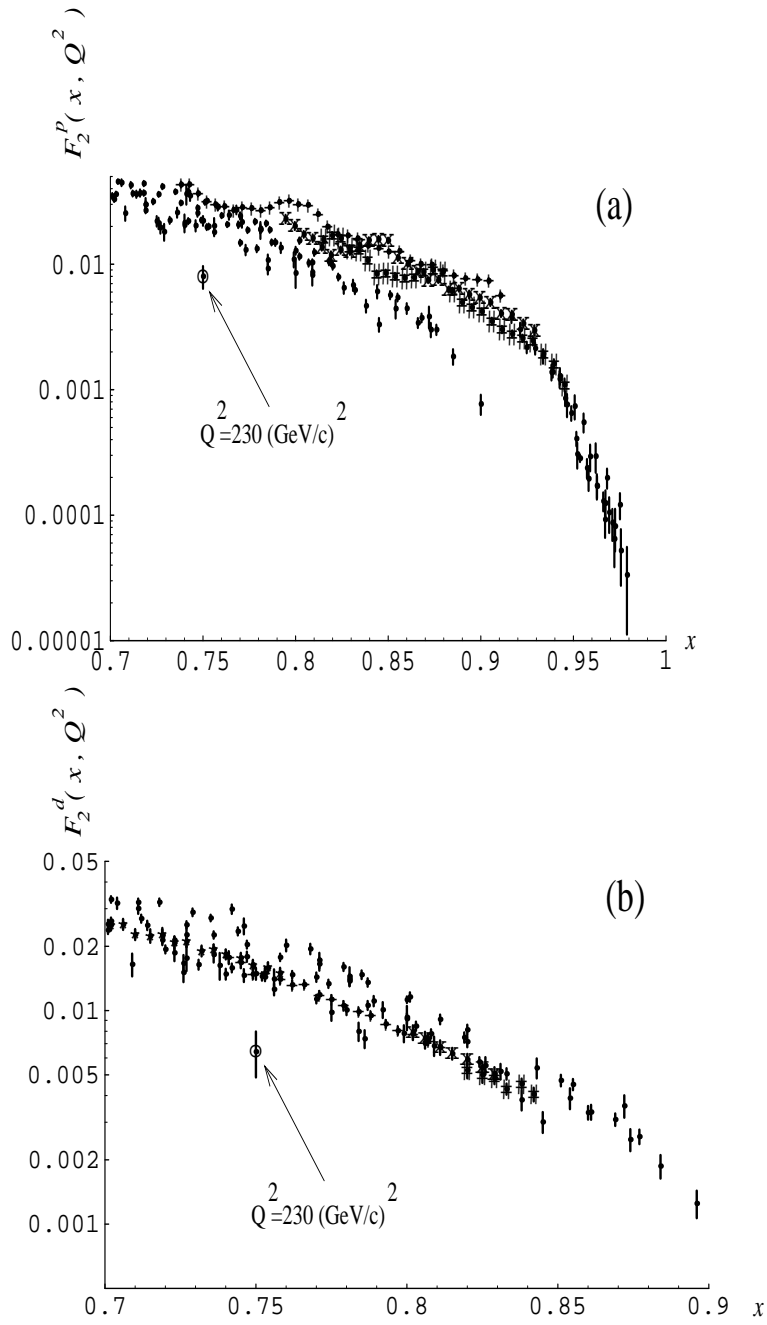


FIG. 2. The SLAC data[5,6,7,8] ($5 \leq Q^2 \leq 30 \text{ (GeV/c)}^2$) for proton (a) and deuteron (b), are shown as a function of the Bjorken variable x . Three high-statistics data sets[7] for $Q^2 \simeq 5.7, 7.6,$ and 9.5 (GeV/c)^2 are marked by “+”, “x”, and “#” respectively. The point at $Q^2 = 230 \text{ (GeV/c)}^2$ and $x = 0.75$ is from ref.[9].

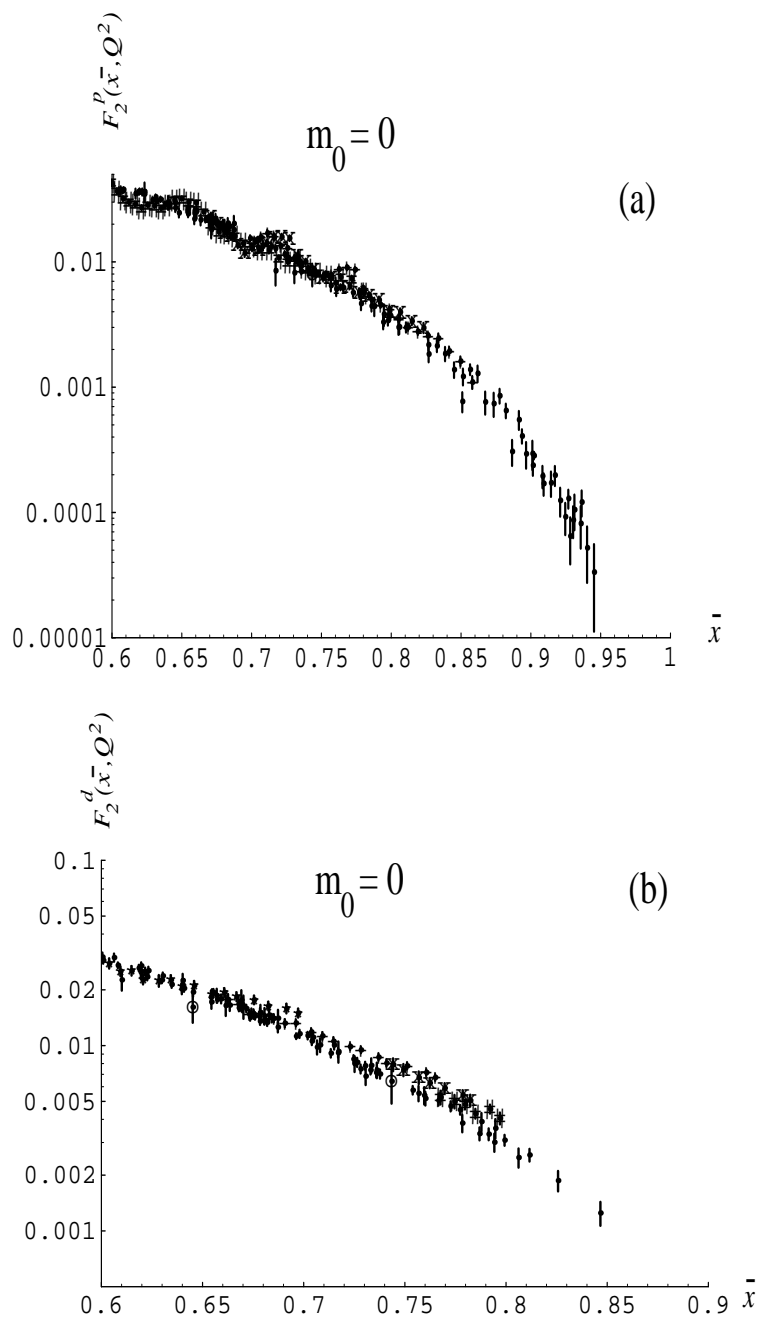


FIG. 3. The data of Fig. 2 are shown as function of the $\bar{x}(x, Q^2)$ —the scaling variable of Eq. (5) — assuming $m_0 = 0$ MeV and $C = 3(\text{GeV})^2$ for the spectator mass m_s , Eq. (7).

On the other hand, the scaling is very good both for the proton and deuteron data, by

taking $m_0 = 0$, i.e. by considering the spectator build up by current quarks [3]. The results are shown in Fig. 3, where the data are plotted as a function of \bar{x} for $m_0 = 0$ and $C = 3 \text{ (GeV)}^2$. Note, that the high- Q^2 data points from BCDMS data [9] are very close to the SLAC data points, taken at much lower values of Q^2 .

Now by using the scaling variable \bar{x} , Eq. (5) for $m_0 = 0$ we can analyze the nucleon structure functions for smaller values of x , where both power and logarithmic corrections to the Bjorken scaling play an important role. In this region ($0.35 < x < 0.75$) the existing BCDMS [9] and NMC [10] data are extended up to much larger values of momentum transfer than the previously considered high- x SLAC data. It allows us to check our predictions in a wide Q^2 range. The results [13] are shown in Figs. 4 and 5 for proton and deuteron structure functions respectively. The data points are from SLAC and BCDMS data bins [5,9]. The dotted lines show the Q^2 -dependence of the structure functions due to power corrections only.

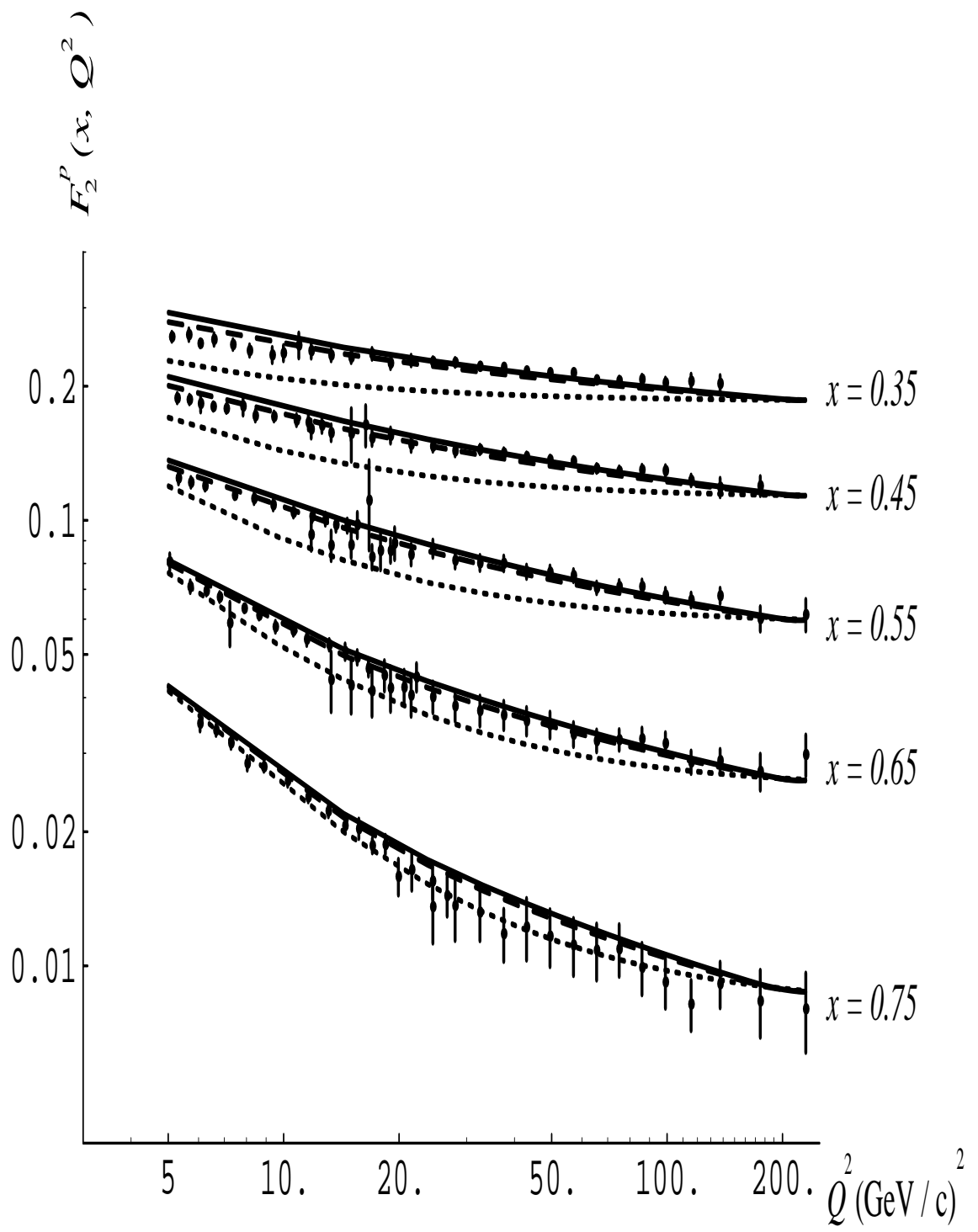


FIG. 4. The proton structure function $F_2^p(x, Q^2)$ is shown as a function of Q^2 at different x -values. The dotted lines include power corrections only. They are evaluated according to and the scaling variable \bar{x} of Eqs. (5), (7) with $m_0 = 0$ and $C = 3 \text{ (GeV)}^2$. The additional QCD logarithmic corrections evaluated at NLO for different Λ scales are shown by the dashed ($\Lambda = 100 \text{ MeV}$) and continuous lines ($\Lambda = 200 \text{ MeV}$).

The total Q^2 -dependence of structure functions due to the power and the logarithmic NLO corrections, is shown by the dashed and continuous lines for $\Lambda = 100 \text{ MeV}$ and $\Lambda = 200 \text{ MeV}$ respectively. The QCD (logarithmic) evolution corrections are taken into account at Next-to-Leading Order (NLO) evolving *back*, in Q^2 , the structure functions starting from an asymptotic value of momentum transfer where the condition $F_2(x, Q^2) \simeq F_2^{as}(x, Q^2)$ (cf. Eq. (1)) is fulfilled (in the present case we choose $Q^2 = 230 \text{ (GeV/c)}^2$, which is the highest value of the momentum transfer in the BCDMS data [9]).

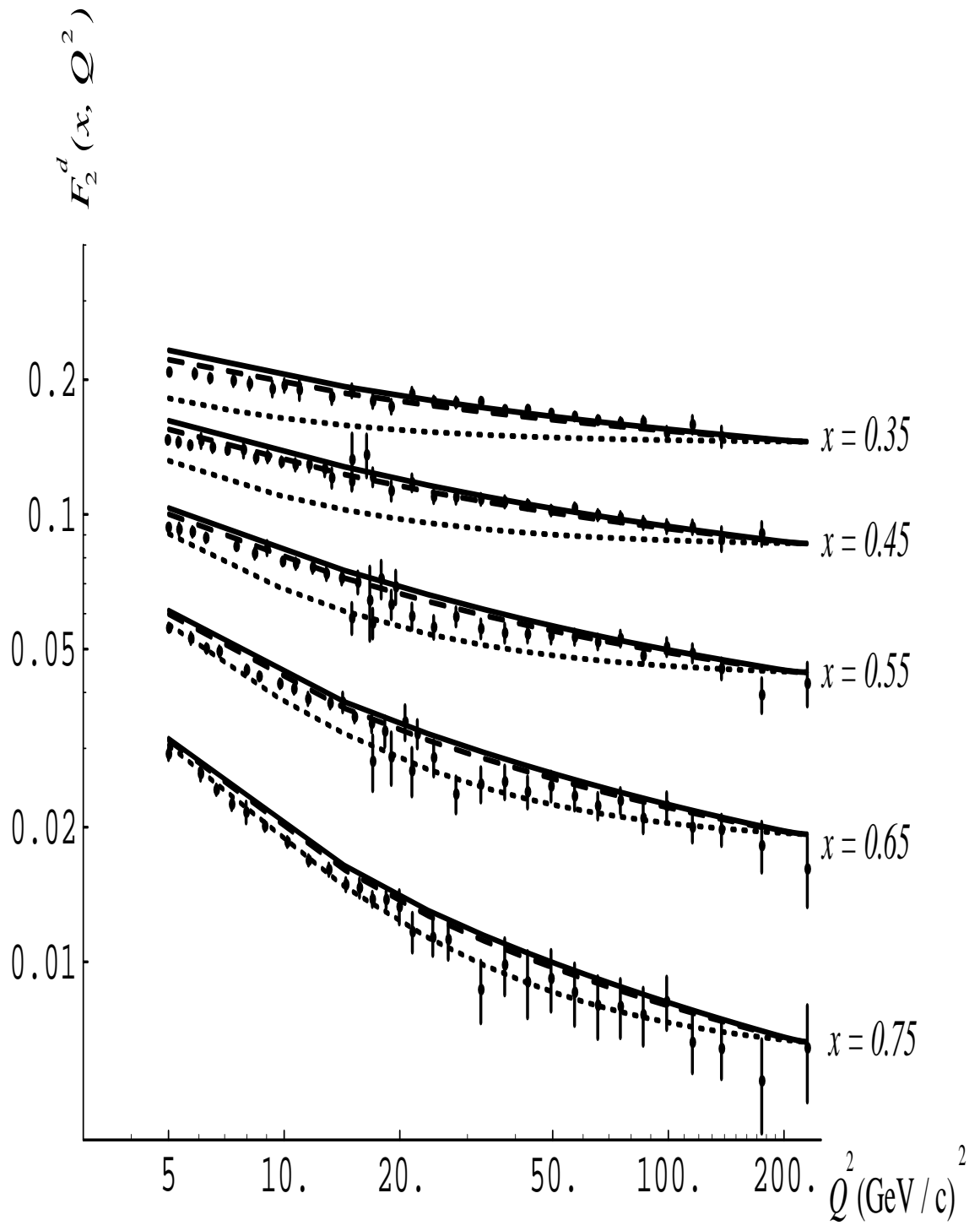


FIG. 5. As in Fig. 4 for the deuteron structure function $F_2^d(x, Q^2)$.

One finds from Figs. 4 and 5 that the experimental data are reproduced in a large Q^2 -range for both values of Λ , although the agreement is slightly better for $\Lambda = 100$ MeV. In addition, since the results are strongly dependent on the spectator mass (7), it is remarkable that the same parameters $m_0 = 0$ and $C = 3$ (GeV)² do reproduce the Q^2 -behavior of the structure functions both for large and moderate x -values.

The above analysis of the nucleon structure functions allows us to extract from data the previously unattainable information on the asymptotic ratio of $F_2^n(x)/F_2^p(x)$ at large x , directly related to u and d -quarks distribution. Indeed, according to the quark-parton model, the structure functions of hadrons in the Bjorken limit ($Q^2 = \mathbf{q}^2 - \nu^2 \rightarrow \infty$ and $x = Q^2/2M\nu = \text{const}$) are directly related to the parton distributions $q_i(x)$. For instance

$$F_2(x, Q^2) \rightarrow F_2(x) = \sum_i e_i^2 x q_i(x), \quad (8)$$

where the sum is over the partons, whose charges are e_i . In the region $x \rightarrow 1$, the contribution of sea quarks can be neglected. Then assuming the same distribution of the valence quarks, one easily finds from Eq. (8) that the neutron-to-proton ratio $F_2^n(x)/F_2^p(x)$ approaches 2/3 for $x \rightarrow 1$. If, however, the quark distributions are different, one can establish only upper and lower limits for this ratio, $1/4 < F_2^n/F_2^p < 4$, which follow from isospin invariance [14].

In order to check the parton model predictions one needs to take the structure functions at high Q^2 , since the higher-twist corrections to the scaling are very important at high- x region. At present, high Q^2 structure functions ($Q^2 \simeq 250$ (GeV/c)²) extracted from BCDMS [9] and NMC [10] data are available only for $x \leq 0.7$. The ratio $F_2^n(x)/F_2^p(x)$ obtained from an analysis of these data [15] shows steady decrease with x . Thus, it is usually assumed that this ratio would reach its lower bound, $F_2^n/F_2^p \rightarrow 1/4$, for $x \rightarrow 1$ (although the recent analysis [16] suggests that this ratio would be larger than 1/4 for $x \rightarrow 1$). This corresponds to $d(x)/u(x) \rightarrow 0$ for $x \rightarrow 1$, where $d(x)$ and $u(x)$ are the distribution functions for up and down quarks in the proton.

Since our scaling variable \bar{x} takes effectively into account the higher-twist corrections, it allows us to reach the asymptotic limit already at moderate values of momentum transfer, $Q^2 < 30$ (GeV/c)². Thus, F_2^p and F_2^d extracted from the SLAC data at large values of x [5–8], Fig. 3, would represent the asymptotic structure functions: $F_2(\bar{x}) = F_2(x) \equiv F_2(x, Q^2 \rightarrow \infty)$, which can be used as an input to determine the ratio $F_2^n(x)/F_2^p(x)$. For this purpose we parametrize the asymptotic structure functions as $F_2^{p,d}(x) = \exp(-\sum_{i=0}^4 a_i x^i)$ and determine the parameters a_i from the best fit to the data in Figs. 3a, 3b. The resulting F_2^n/F_2^p ratio is shown in Fig. 6 by the solid line. The dotted lines are the error bars on the fit, which combine statistical and systematic uncertainties. The dashed line corresponds to $F_2^n/F_2^p = 2/3$. For a comparison, we show by the dot-dashed line a polynomial extrapolation of this ratio to large x , obtained from BCDMS and NMC data by assuming that $F_2^n/F_2^p \rightarrow 1/4$ for $x \rightarrow 1$ [15]. structure functions

$$F_2^n(x)/F_2^p(x)$$

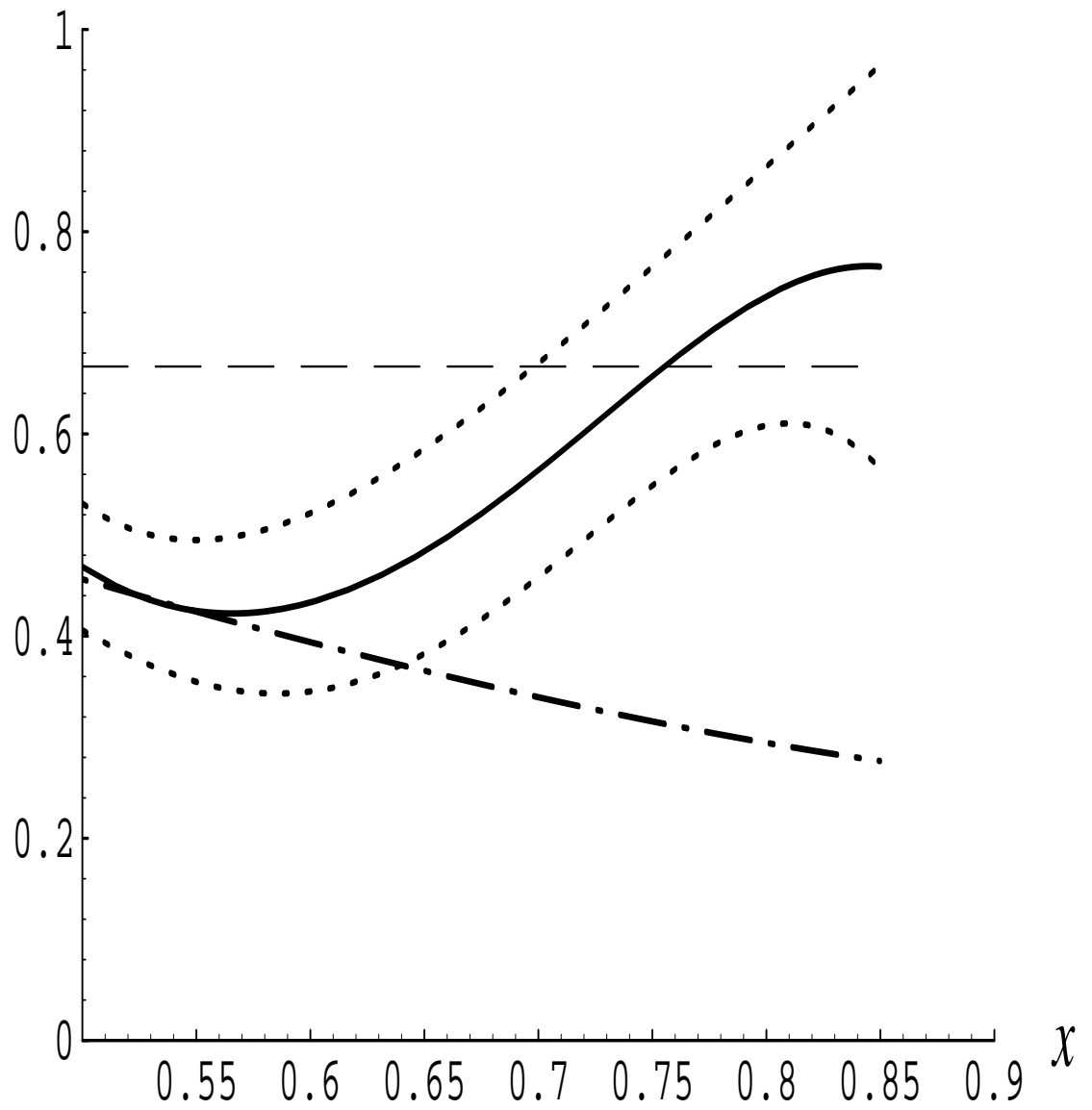


FIG. 6. Neutron-to-proton structure function ratio at large x .

Our results shown in Fig. 6 demonstrate that contrary to earlier expectations, the ratio F_2^n/F_2^p does not approach its lower bound, but increases up to approximately $2/3$. The latter is the quark model prediction, assuming the same distributions for each of the valence quarks. The accuracy of our results will be checked in future experiments, which will provide high Q^2 data for the structure functions at large x .

The described above method for evaluation of the higher-twist corrections using modified scaling variable can be very useful for not only for an analysis of high- x nucleon structure functions, but also for a treatment of many different problems, where the interaction of partons in the final state becomes important. In particular, I would like to mention the sum rules, where the role of higher-twist effects remains an open problem, and the structure functions at $x \rightarrow 0$. In this region the spectator mass m_s is not described by Eq. (7), valid for large x . If $m_s^2 \propto 1/Q^2$ for $x \rightarrow 0$, then $(\bar{x} - x)/x \propto 1/Q^2$, Eq. (5), and the role of higher-twist correction would be substantial in this region too.

REFERENCES

- [1] O.W. Greenberg, Phys. Rev. D**47**, 331 (1993);
- [2] S.A. Gurvitz and A.S. Rinat, Phys. Rev. C**47**, 2901 (1993).
- [3] S.A. Gurvitz, Phys. Rev. D**52**, 1433 (1995).
- [4] R.L. Jaffe, in *Los Alamos School on Relativistic Dynamics and Quark-Nuclear Physics*, ed. M.B. Jackson and A. Picklesimer. (John Wiley and Sons, New York, 1985).
- [5] L.W. Whitlow, Ph.D. Thesis, Stanford University, 1990, SLAC-REPORT-357 (1990).
- [6] L.W. Whitlow *et al.*, Phys. Lett. B**282**, 475 (1992).
- [7] S.E. Rock *et al.*, Phys. Rev. D**46**, 24 (1992).
- [8] P.E. Bosted *et al.*, Phys. Rev. D**49**, 3091 (1994).
- [9] BCDMS Collab., A.C. Benvenuti *et al.*, Phys. Lett. B**223**, 485 (1989); Phys. Lett. B**237**, 592 (1989).
- [10] NMC Collab., P. Amaudruz *et al.*, Phys. Lett. B**295**, 159 (1992).
- [11] W. Melnitchouk, A.W. Schreiber and A.W. Thomas, Phys. Lett. B**335**, 11 (1994).
- [12] Similar small binding and Fermi motion effects in the deuteron structure function were also found in a recent phenomenological analysis of J. Gomez *et al.*, Phys. Rev. D**49**, 4348 (1994).
- [13] S.A. Gurvitz, A. Mair and M. Traini, Phys. Lett. B, in press.
- [14] O. Nachtmann, Nucl. Phys. B**38**, 397 (1972).
- [15] BCDMS Collab., A.C. Benvenuti *et al.*, Phys. Lett. B**237**, 599 (1989).
- [16] W. Melnitchouk and A.W. Thomas, Phys. Lett. B**377**, 11 (1996).